Application of Nuclear Microprobe in Biomedical, Industrial and Fusion Research

P. Vavpetič, N. Grlj, P. Pelicon

**Jožef Stefan Institute, Association EURATOM-MHEST,
Jamova 39, SI-1000, Ljubljana, Slovenia**

Microbeam instrumentation at JSI

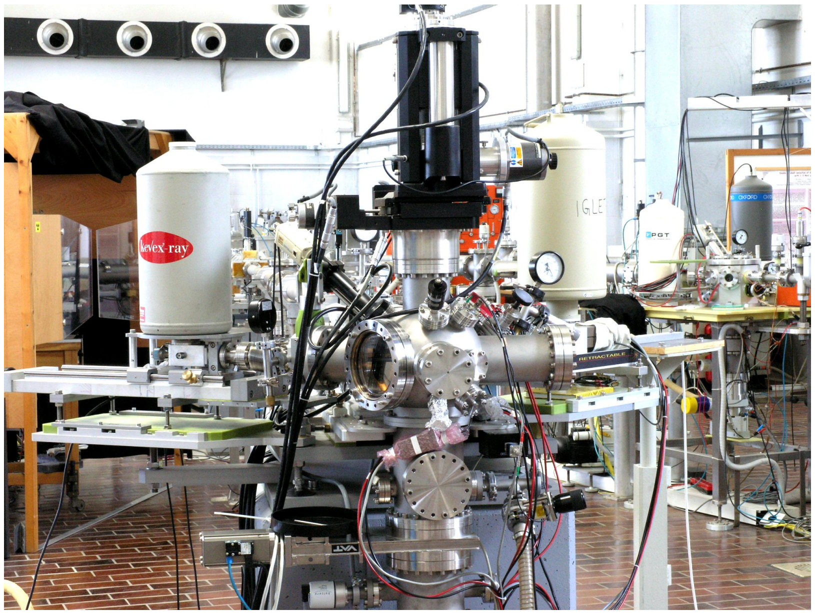

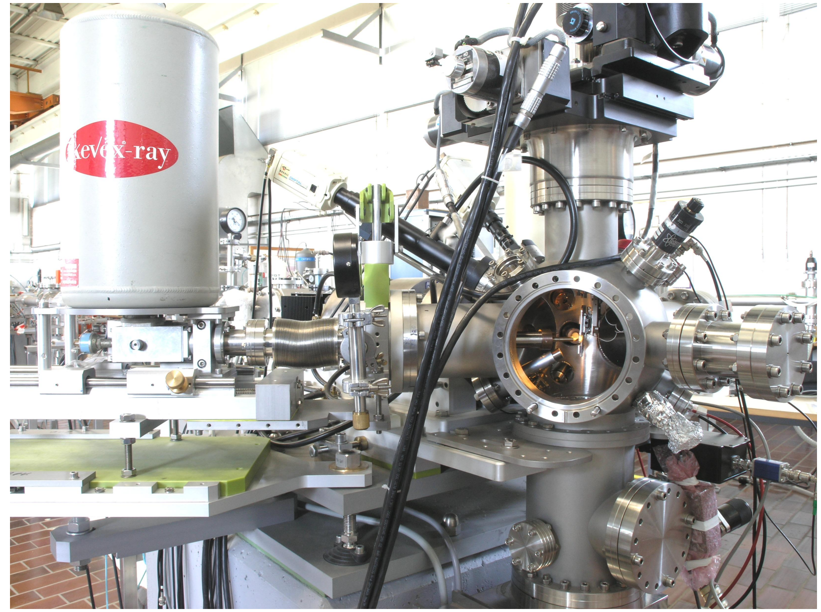

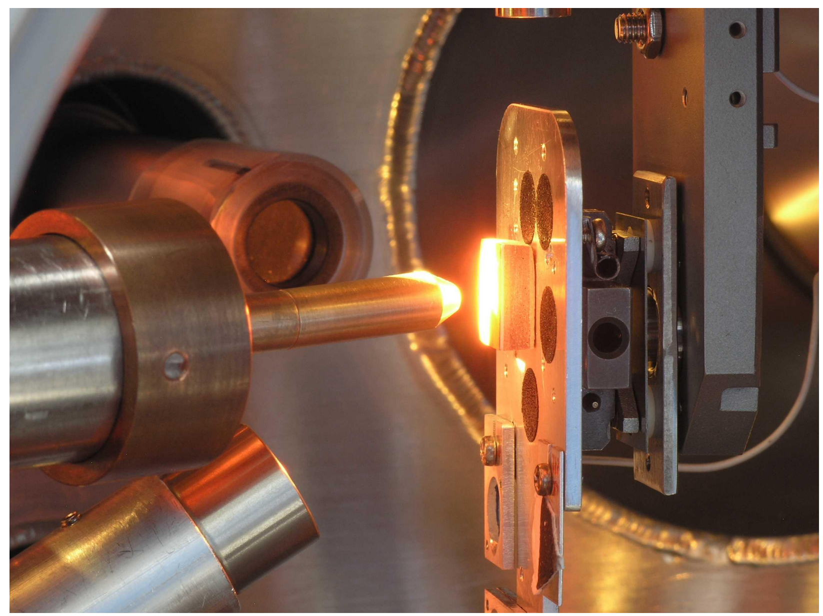

Microbeam schematics at JSI

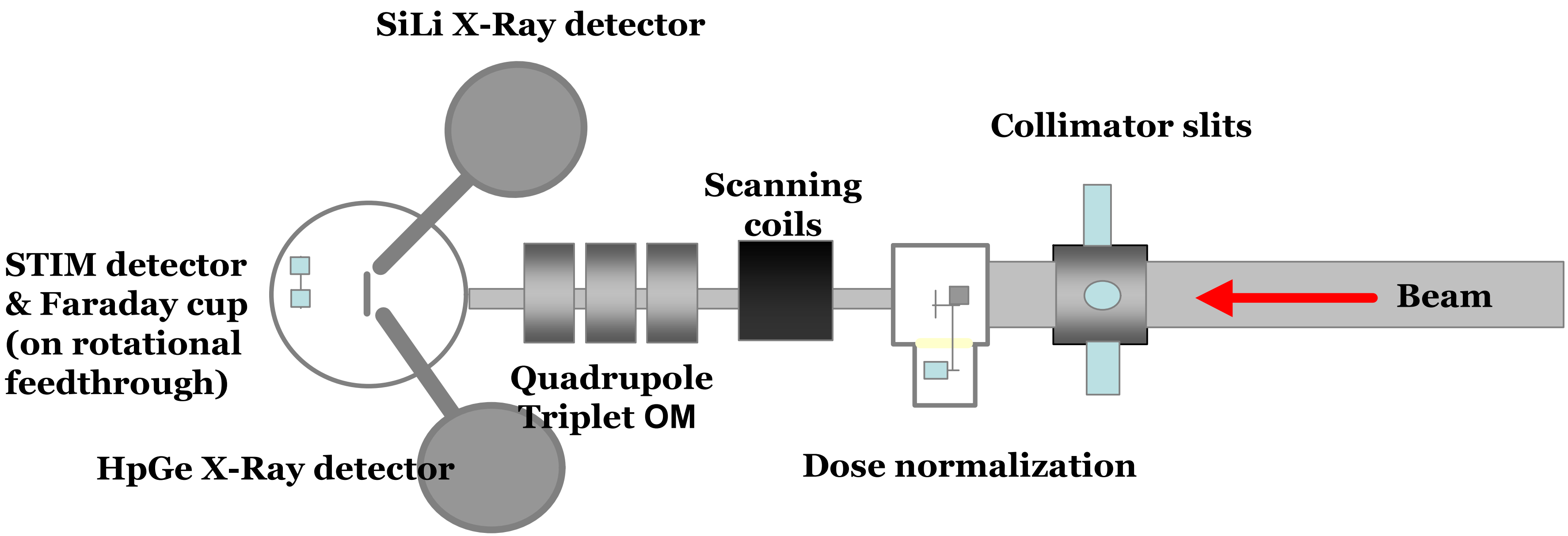

Ion microbeam dose normalization:

RBS from Au coated graphite chopper is sampled simultaneously with other spectra (PIXE, RBS, SE, STIM, ERDA…)

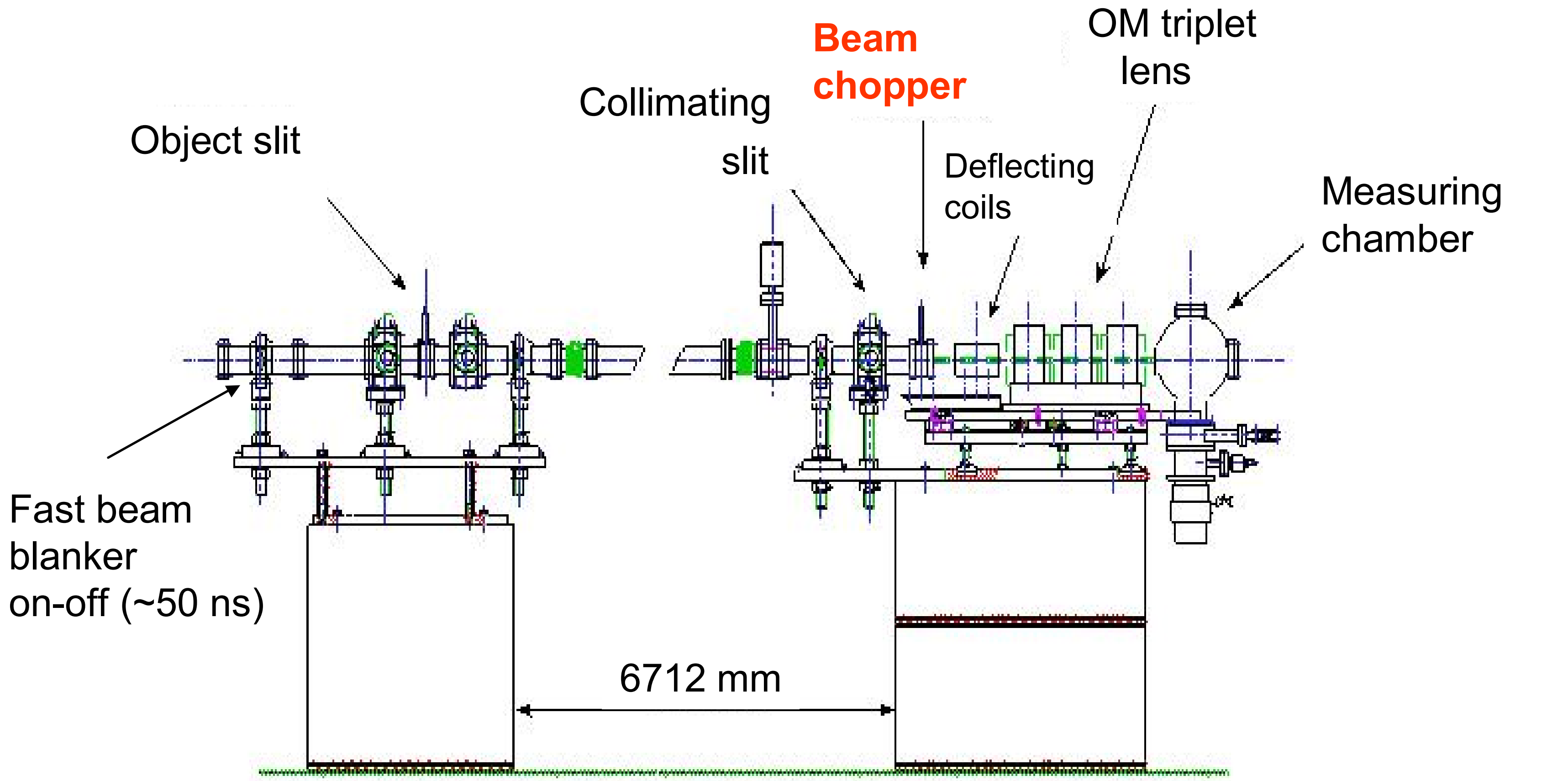

Dose normalisation for quantitative analysis: RBS from rotating chopper positioned in the beam after the collimation slits

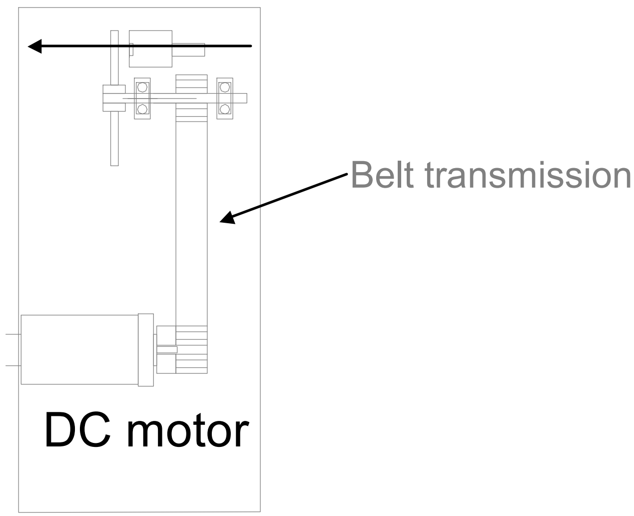

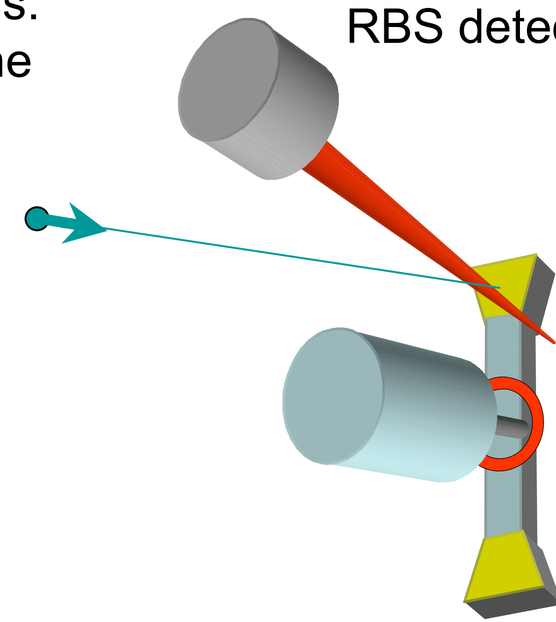

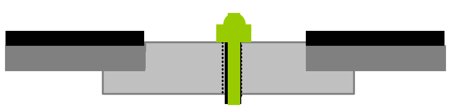

3x1 μm thick gold foil on graphite, mounted on aluminium support

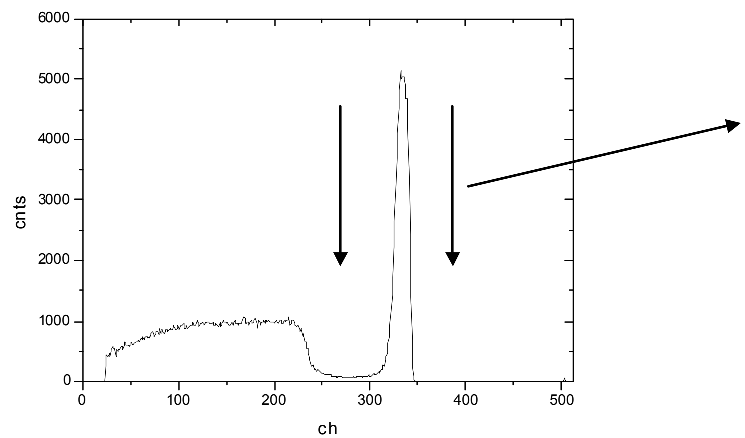

Integrated Au signal proportional to the proton dose

Fusion-related research

-^{7}Li beam, 3 - 4.5 MeV for ERDA, RBS, LIXE
-^{3}He beam, 0.5 – 2 MeV for NRA

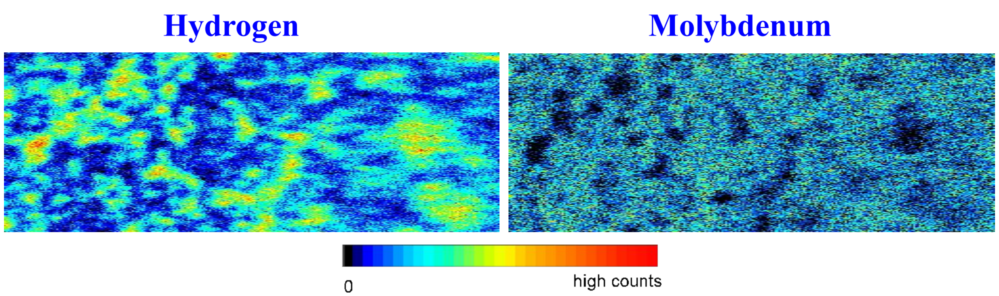

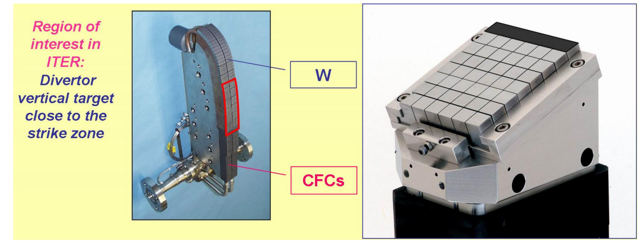

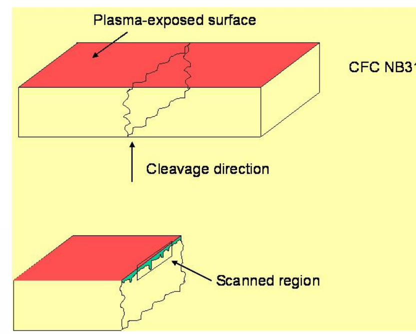

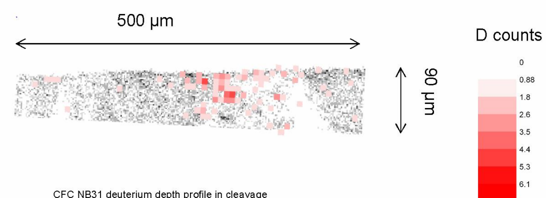

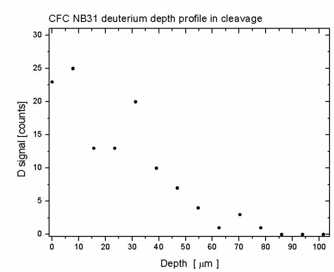

Areal distribution of hydrogen and molybdenum measured simultaneously by ERDA and Li-beam excited X-ray emission (LIXE) over an area of 1240 x 450 µm2 (top). The surface belongs to a graphite section of the castellation limiter [1] (top right) exposed inside the plasma of TEXTOR tokamak, IPP Juelich. Molybdenum originates from re-deposition process from castellation sections made of molybdenum. Hydrogen and molybdenum surface concentrations are anti-correlated. Deuterium depth profiles in Carbon Fiber Composite materials exposed to deuterium plasma inside TEXTOR tokamak [2] (right).

[1] A. Litnovsky et al, J. Nucl. Mater. 337-339, 917 (2005)
[2] A. Kreter et al., Phys. Scr. T128, 35 (2007) .

Biomedical research

- p beam, 3 MeV for PIXE, STIM…

Tissue elemental mapping and quantification sequence*:

1. **Area selection (fast, PIXE)**

2. **0º STIM – list mode (500 Hz)**

3. **PIXE mapping, long – list mode (100-500 pA, 1-2.5 μm beam)**

4. **0º STIM – list mode, low current, beam damage control**

5. **Off-line area selection, extraction of average thickness, fed in GUPIXWIN as exit energy, matrix assumed (i.e. cellulose for dry plant samples), GUPIXWIN trace calculation**

***Green does not apply for thick samples**

Recent micro-PIXE biomedical research at JSI :

1. **Localisation of Cd, Zn, Pb inCd/Zn hyperaccumulator *Thlaspi praecox Wulfen* (*Vogel-Mikuš et al., Env. Pollution 2007, Plant, Cell, Environment 2008*).**
2. **Elemental redistribution in lichens after arsenate exposure (*Mrak et al, 2007*).**
3. **Forestry: year pattern elemental distribution in wood, branch recovery and reaction zone mapping after cutting (Merela et al. in print NIMB).**
4. **Penetration of TiO_2 nanoparticles through biomembranes.**
5. **Buckwheat: elemental distribution in seed after Zn soil treatment.**
6. **Halophytes (plants growing in saline-rich environment).**
7. **Elemental distribution of mercury in human tissue after long term mercury exposure.**
8. **Uranium treated Arabidopsis plant**
9. **Viola westfalica in polluted and unpolluted soil**
10. **Ordinary wheat: elemental distribution in seed**

Cryofixation,freeze drying

Developed with Biotechnical faculty UL in collaboration with Heidelberg group
Schneider et al, IJ PIXE 12, 101 (2002).

Cutting the tissue with a stainless steel razor blade

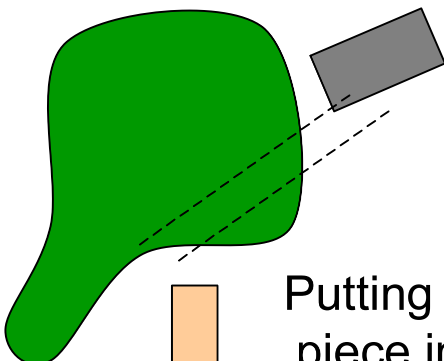

Putting the piece into 2 mm needle

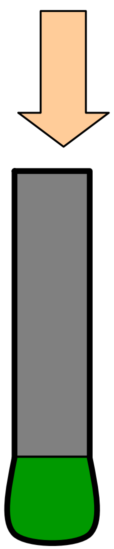

Rapid freezing

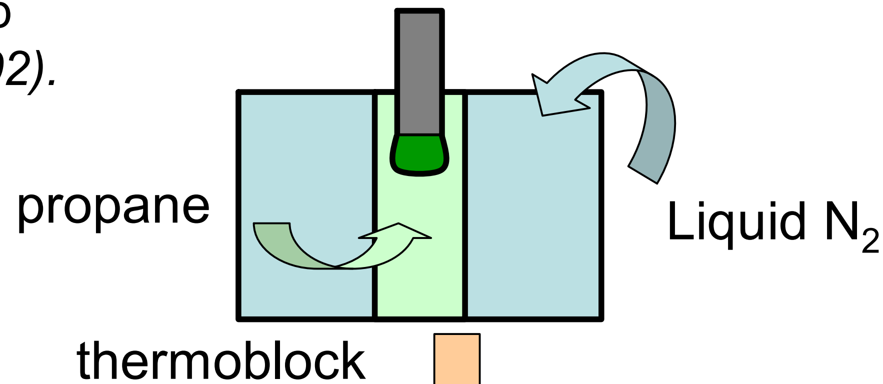

Cutting with cryotome

Freeze-drying

Mounting on a holder between two layers of pioloform (formvar) foils

***Thlaspi praecox* Wulf.**
Brassicaceae

- **Hyperaccumulation of Cd and Zn**
  Exclusion of Pb

Žerjav, Slovenia

Total soil conc.

- **50 000 ppm Pb**
- **3 500 ppm Zn**
- **200 ppm Cd**

SO_2 emissions

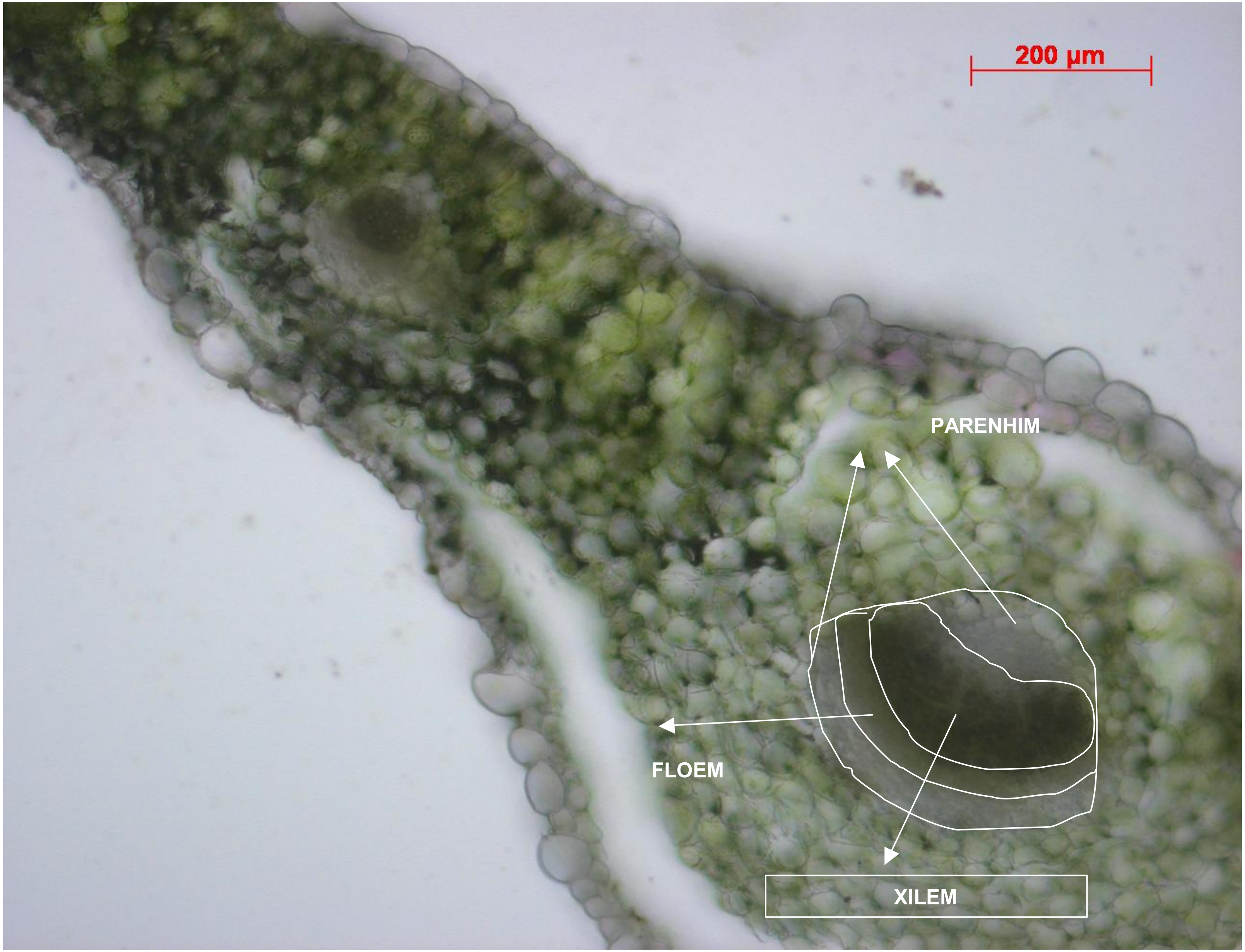
200 µm
PARENHIM
FLOEM
XILEM

Thlaspi leaf 2000 x 2000 µm^2

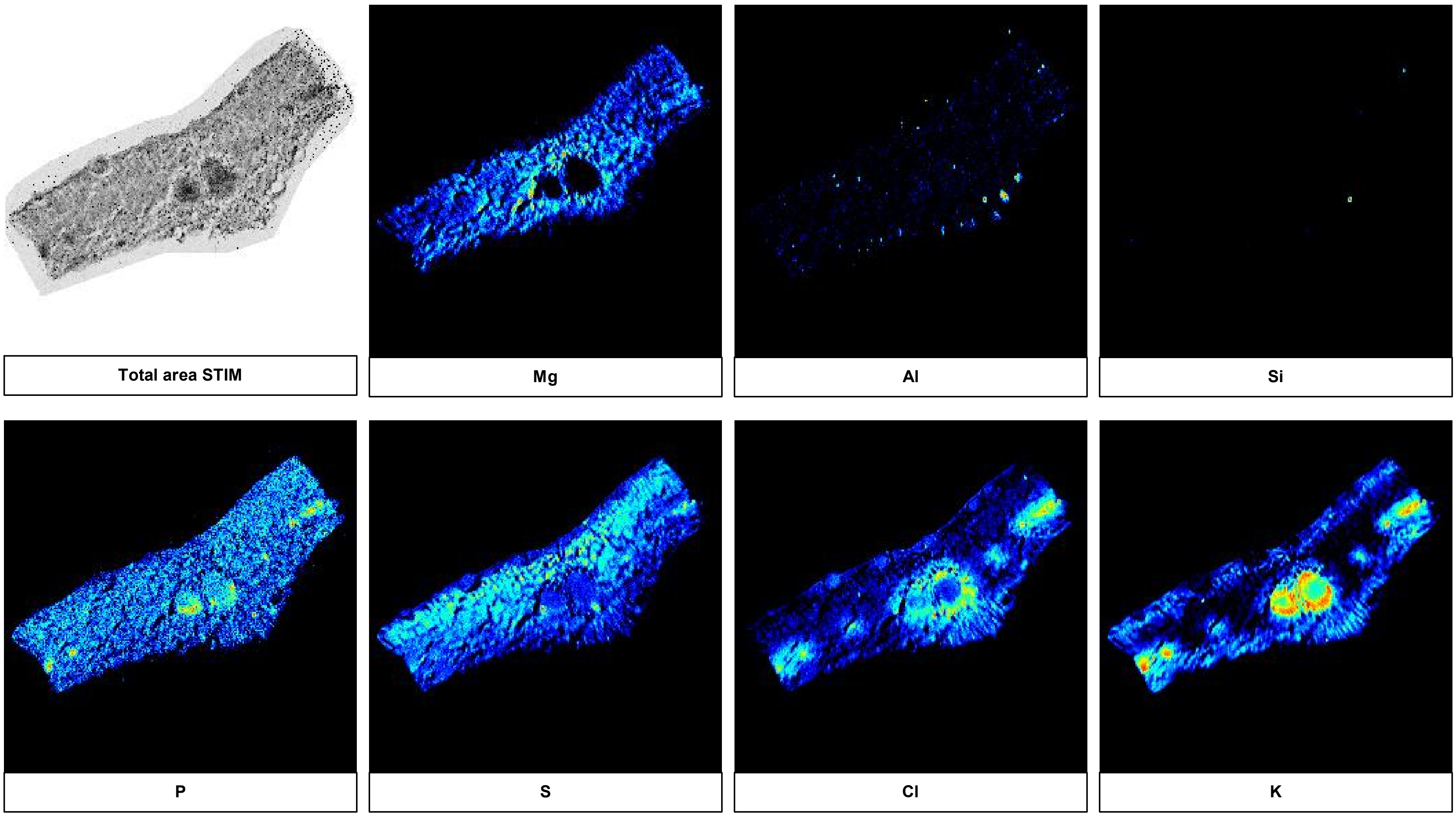

Thlaspi leaf 2000 x 2000 μm²

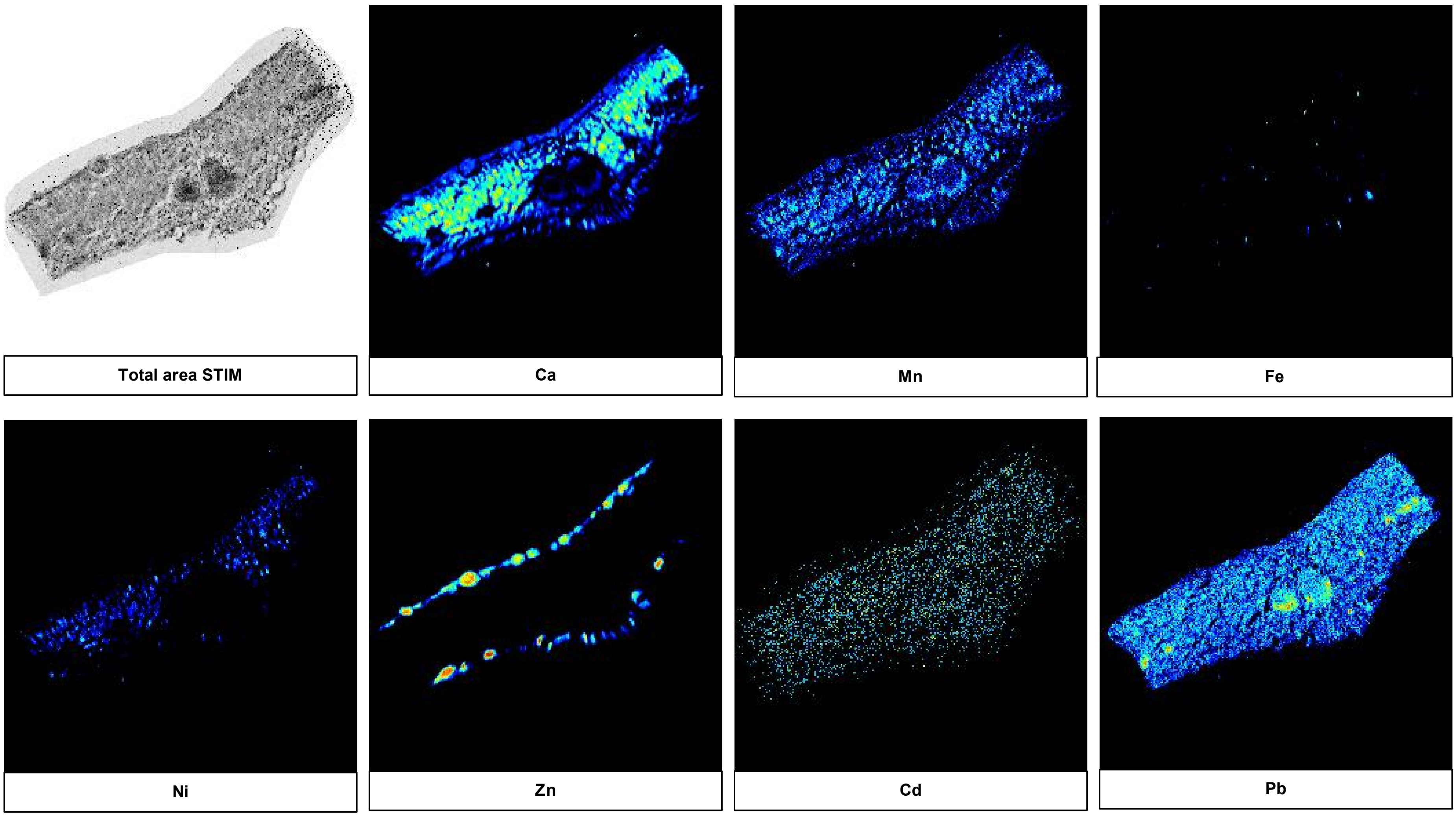

Zoom, scan size 500 µm x 500 µm

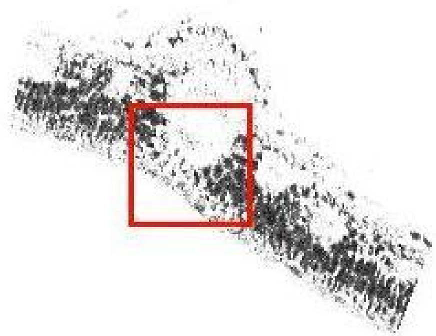

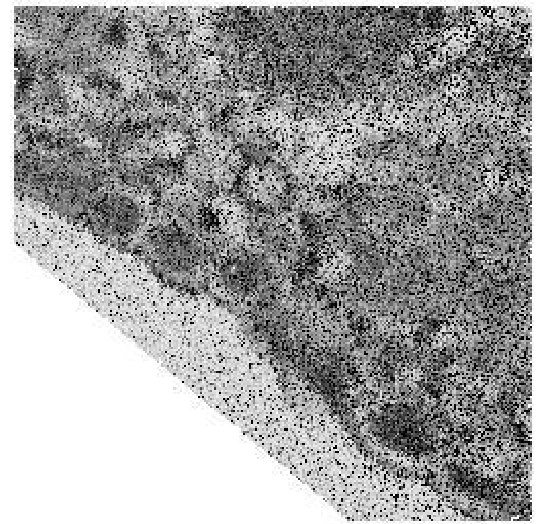

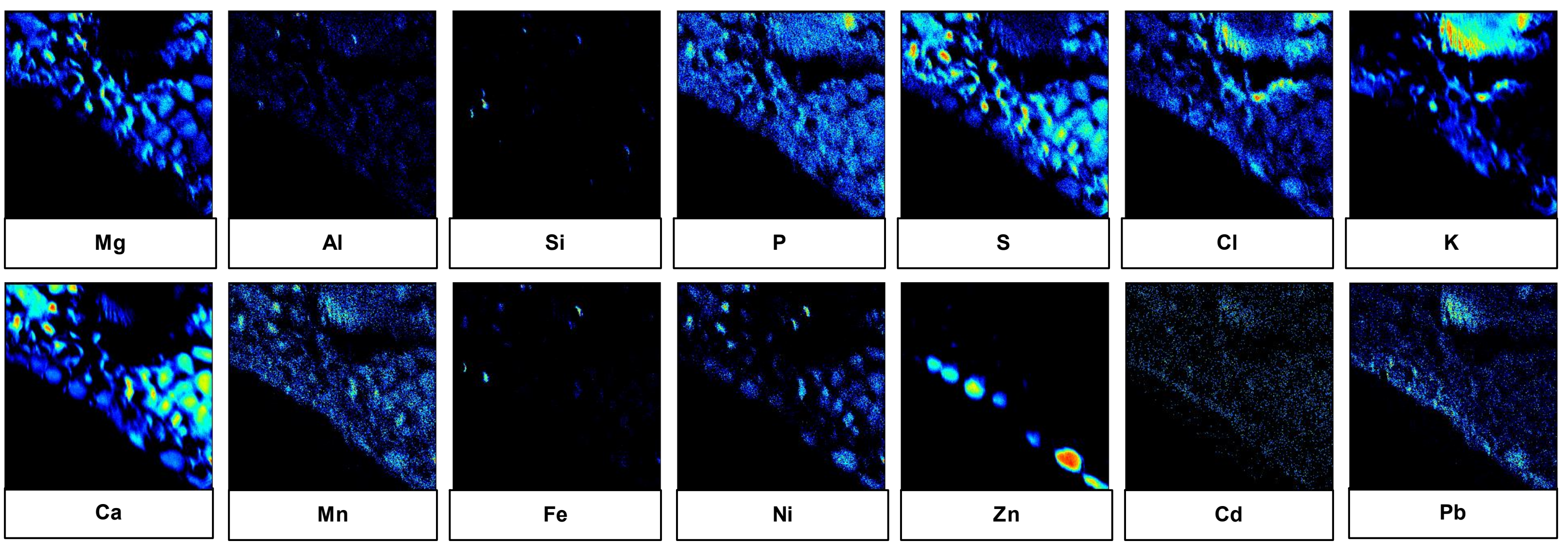

Zoom, scan size 500 µm x 500 µm

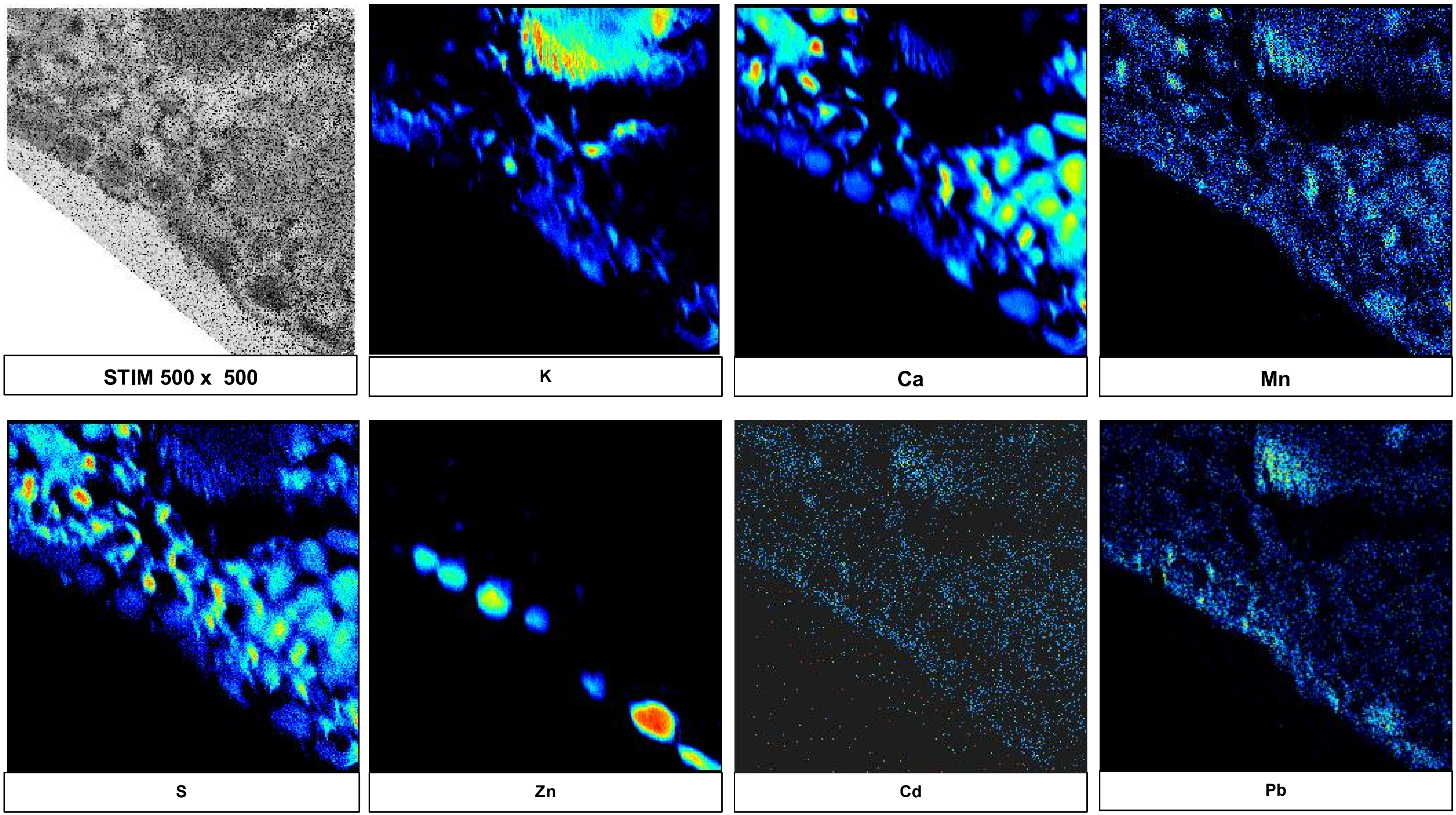

Micro-PIXE: Scanned area 2040 x 2040 μm^2

Whole area	Upper epidermis	Palisade mesophyll	Vascular bundle	Spongy mesophyll	Lower epidermis
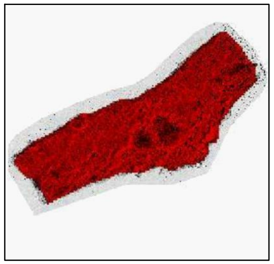	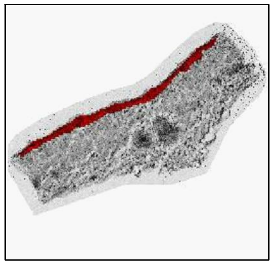	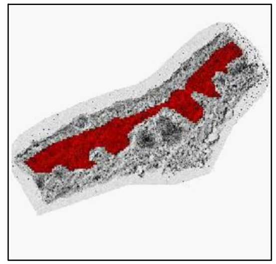	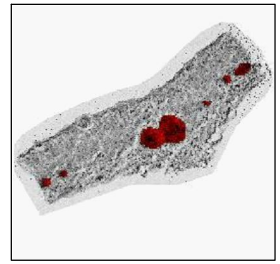	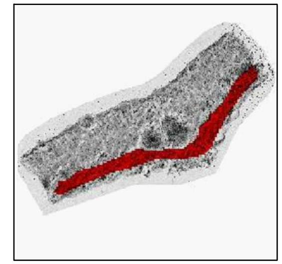	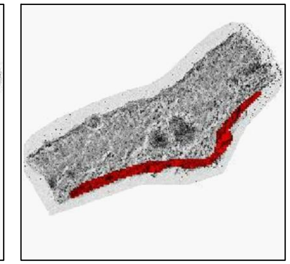

	Whole area			Upper epidermis			Palisade mesophyll			Vascular bundle			Spongy mesophyll			Lower epidermis		
El.	$\mu g\ g^{-1}$	Error (%)	LOD	$\mu g\ g^{-1}$	Error (%)	LOD	$\mu g\ g^{-1}$	Error (%)	LOD	$\mu g\ g^{-1}$	Error (%)	LOD	$\mu g\ g^{-1}$	Error (%)	LOD	$\mu g\ g^{-1}$	Error (%)	LOD
P	**1048**	1.61	31.2	**659.4**	6.54	79.0	**802.8**	3.69	57.2	**1868**	2.24	68.9	**1262**	3.61	81.4	**935.7**	5.04	84.9
S	**6209**	0.28	23.3	**3862**	1.23	66.8	**8243**	0.40	39.3	**3218**	1.32	62.8	**6349**	0.82	72.3	**3541**	1.47	79.0
Cl	**5229**	0.36	22.4	**2754**	1.69	66.6	**2831**	0.97	36.6	**7109**	0.75	62.3	**8150**	0.73	70.8	**5745**	1.05	77.7
K	**18412**	0.22	49.4	**9595**	0.92	103.2	**7402**	0.72	78.9	**37378**	0.35	87.9	**28594**	0.42	110	**20633**	0.59	119.4
Ca	**48782**	0.15	70.7	**28983**	0.48	103.5	**84040**	0.15	67.2	**7615**	1.53	180.7	**42938**	0.4	164.5	**31638**	0.53	152.4
Mn	**89.2**	2.73	4.50	**91.5**	6.39	10.3	**83.1**	5.91	9.10	**86.6**	6.67	10.6	**96.4**	6.87	12.1	**104**	6.97	12.9
Fe	**94.2**	3.30	5.8	**79.2**	8.59	12.5	**69.5**	8.55	11.3	**70.0**	10.3	12.9	**107.5**	7.53	14.7	**438.3**	2.31	15.8
Ni	**8.40**	90.2	13.7	**398.6**	2.70	15.7	**n.d.**	n.d	n.d	**8.40**	41.0	6.20	**42.3**	23.1	17.4	**298.4**	4.00	19.2
Cu	**22.2**	10.4	4.10	**58.9**	25.2	27.7	**14.3**	23.9	6.00	**9.50**	31.9	5.50	**17.1**	26.5	7.90	**59.3**	22.5	24.3
Zn	**14102**	0.10	3.00	**64786**	0.16	16.6	**4627**	0.33	4.80	**1054**	1.14	5.60	**8765**	0.39	4.50	**52590**	0.19	22.5
Cd	**2125**	3.88	124.4	**3020**	8.95	348.1	**2372**	6.66	213.6	**2242**	8.80	191.4	**1665**	14.49	342.3	**2099**	14.3	444.2
Pb	**628**	1.73	15.8	**636.2**	7.72	79.5	**357.8**	4.65	26.1	**656.9**	3.91	20.3	**722.4**	4.44	40.7	**1282**	4.50	85.9

Vogel-Mikuš et al, Plant, Cell, Environment (2008)

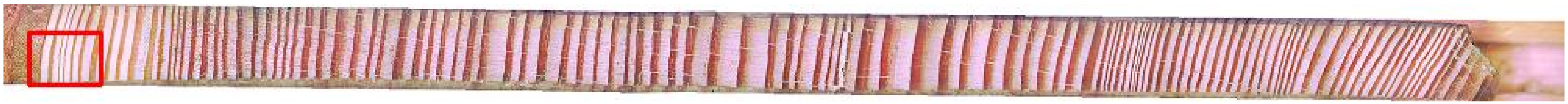

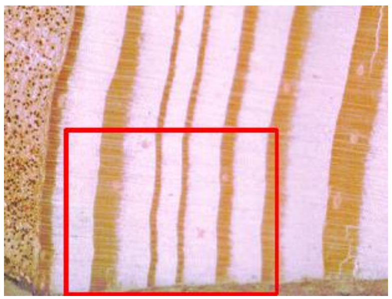

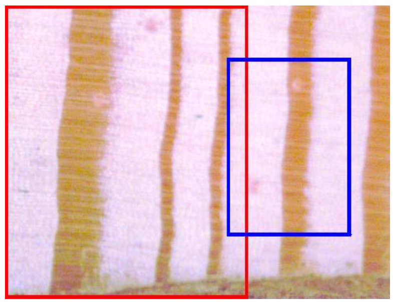

European larch (*Larix decidua* Miller), unpolluted forest, growth ring structure late *vs.* early wood, thick target

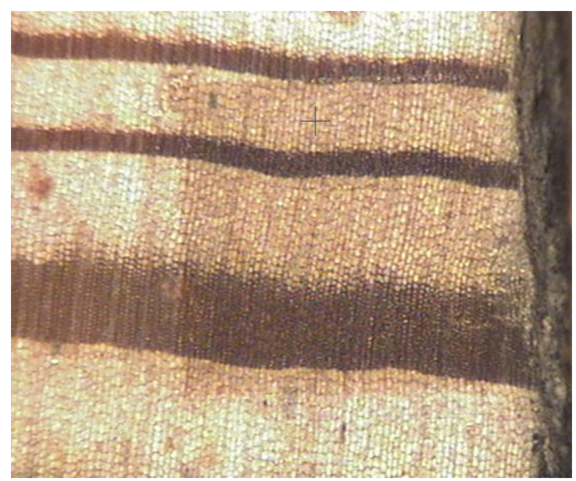

Annual rings from 2003 - 2005

Scan size: 2000 µm x 2000 µm

Scan area

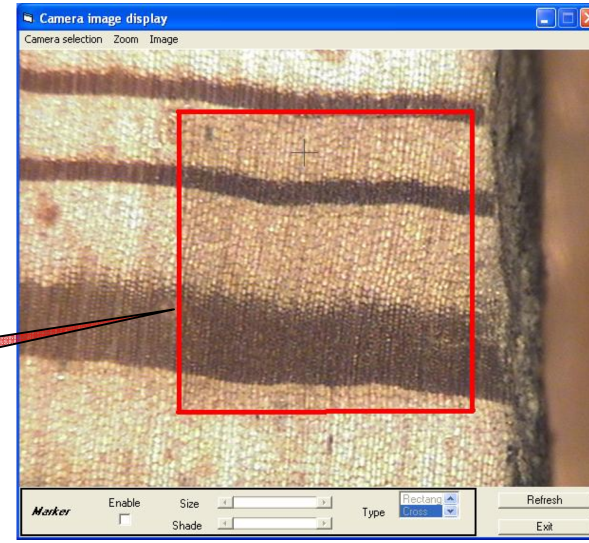

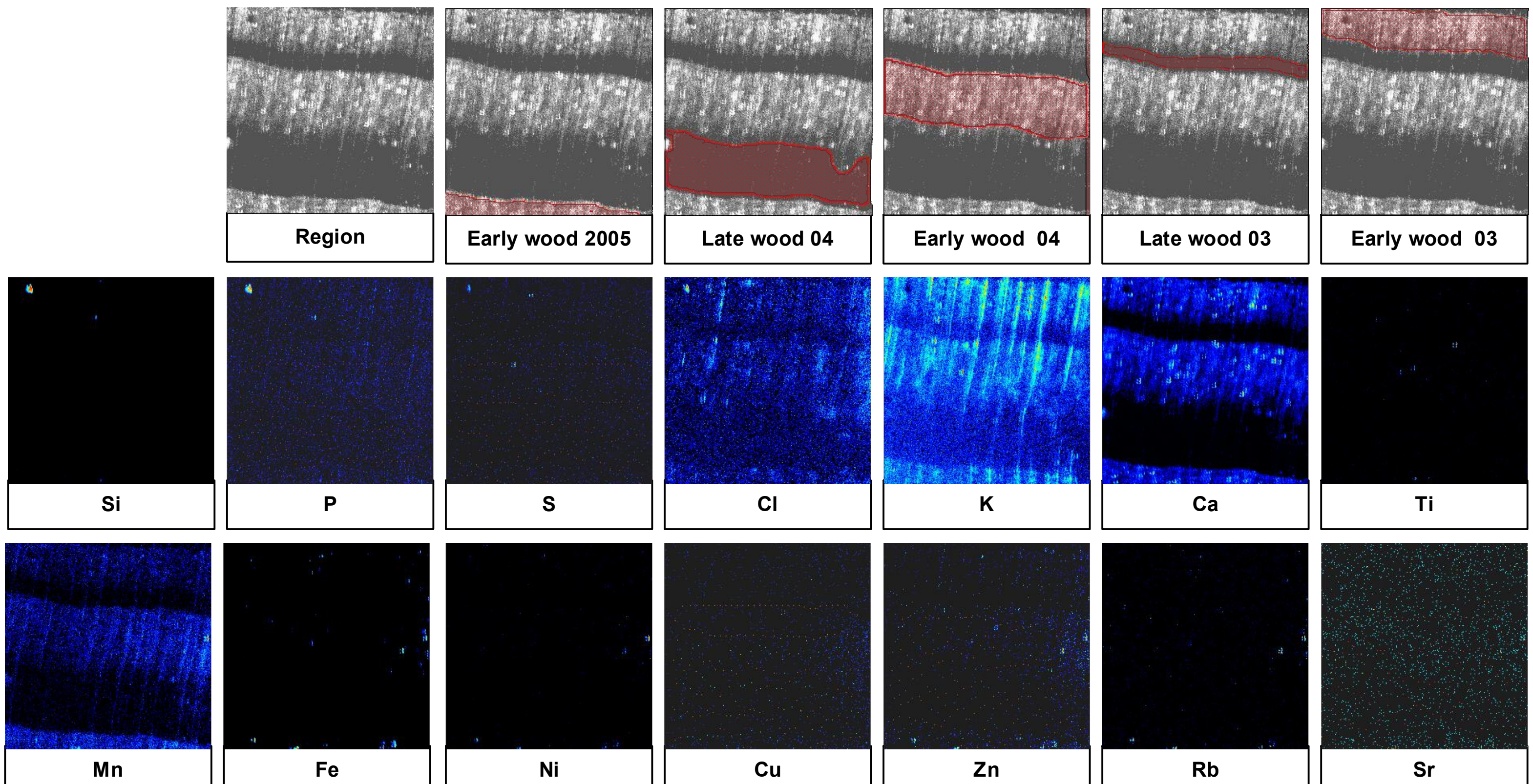

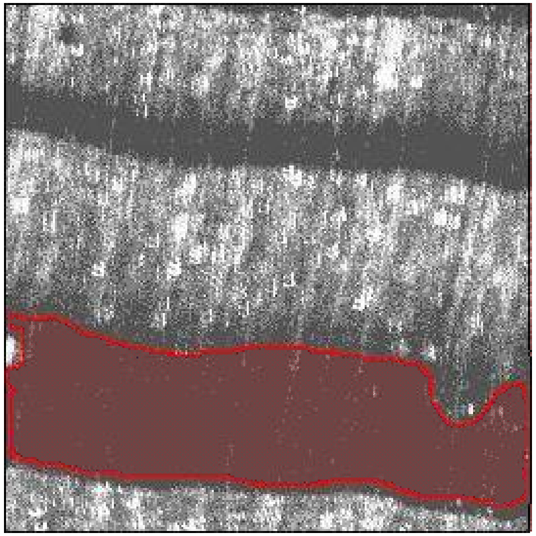

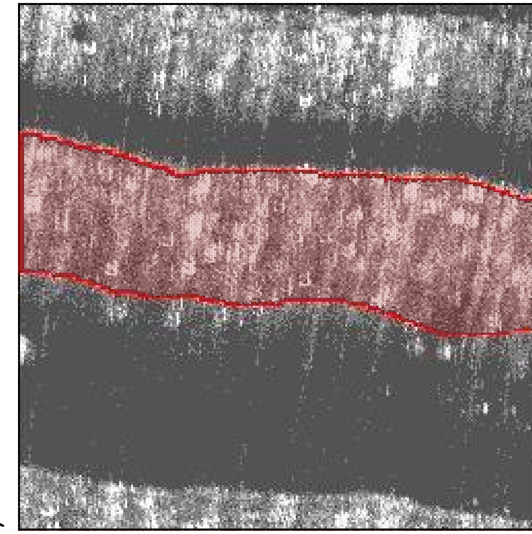

Elementi	Konc [ppm]	Stat.err. %	lod [ppm]
Si	165.7	5.2	15.9
P	176.5	4.94	16.3
S	51.9	11.38	11.1
Cl	62.5	7.92	9.2
K	232.8	1.78	7.1
Ca	295.5	1.31	6.3
Ti	7.40E-01	75.28	1
Cr	0	0	1
Mn	70.5	0.54	4.34E-01
Fe	19.7	2	7.64E-01
Ni	4.68E-01	28.82	2.49E-01
Cu	4.3	3.85	2.39E-01
Zn	3.6	4.54	2.25E-01
Rb	9.20E-01	61.26	1.1
Sr	3.1	24.63	1.3

Elementi	Konc [ppm]	Stat.err. %	lod [ppm]
Si	598.3	1.51	15.9
P	302.6	2.97	16.5
S	182	3.31	11
Cl	287	1.81	9.2
K	600.9	0.76	7.2
Ca	1218.3	0.45	7.3
Ti	24.6	2.26	1
Cr	3.7	9.13	6.22E-01
Mn	143.6	0.35	4.94E-01
Fe	355.5	0.27	1
Ni	2.9	5.81	2.88E-01
Cu	12.9	1.77	2.84E-01
Zn	10.3	2.27	2.85E-01
Rb	5.3	13.81	1.2
Sr	12	7.48	1.3

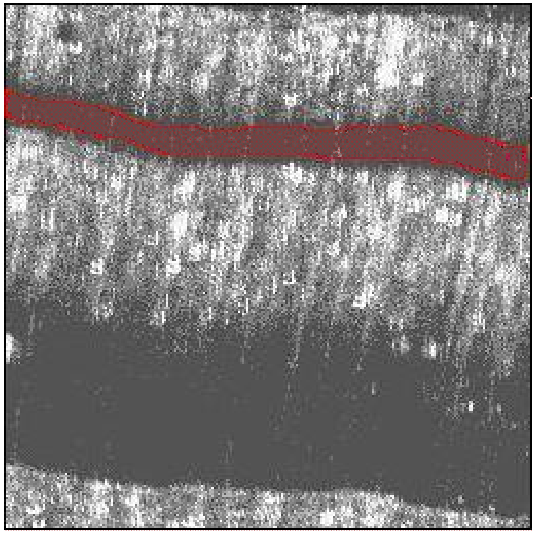

Elementi	Konc [ppm]	Stat.err. %	lod [ppm]
Si	182.3	9.72	32.6
P	227.2	7.9	33.2
S	79.9	15.31	22.8
Cl	88.9	11.65	19.3
K	332.9	2.67	14.9
Ca	313.7	2.54	13
Ti	3.75E-01	311.4	2.2
Cr	0	0	2.1
Mn	60.8	1.23	9.20E-01
Fe	25.6	2.68	1.2
Ni	9.23E-01	29.87	4.80E-01
Cu	2.5	12.6	5.04E-01
Zn	3.3	9.74	3.12E-01
Rb	2.5	47.78	2
Sr	4.6	34.27	2.2

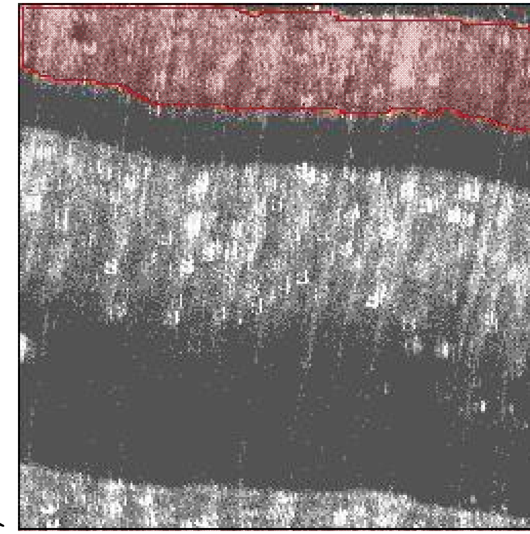

Elementi	Konc [ppm]	Stat.err. %	lod [ppm]
Si	3974.7	0.4	22.8
P	213.8	5.9	22.7
S	174.7	4.53	14.6
Cl	318.5	2.14	12
K	854.3	0.76	9.6
Ca	1276.6	0.57	9.8
Ti	25.9	2.58	1.2
Cr	1.3	30.38	7.33E-01
Mn	109.8	0.49	5.67E-01
Fe	332.6	0.31	1
Ni	2	9.82	3.36E-01
Cu	5	4.25	3.07E-01
Zn	7.8	3.17	3.01E-01
Rb	5.4	14.57	1.3
Sr	10.1	10.32	1.3

Buckwheat grain

***(french:** saracen, **italian:** grano saraceno, **german:** Buchweizen**, in Japan:** soba nudles,…)*

Dry buckwheat and many others seeds are hard.
Not possible to slice with cryotome.
“Thick target” micro-PIXE
Seed envelope mapping and quantification: geometry, absorption !

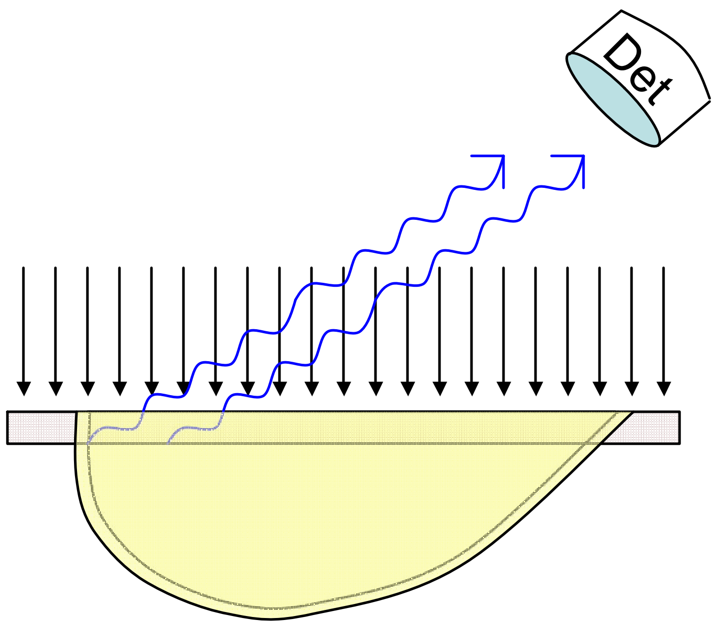

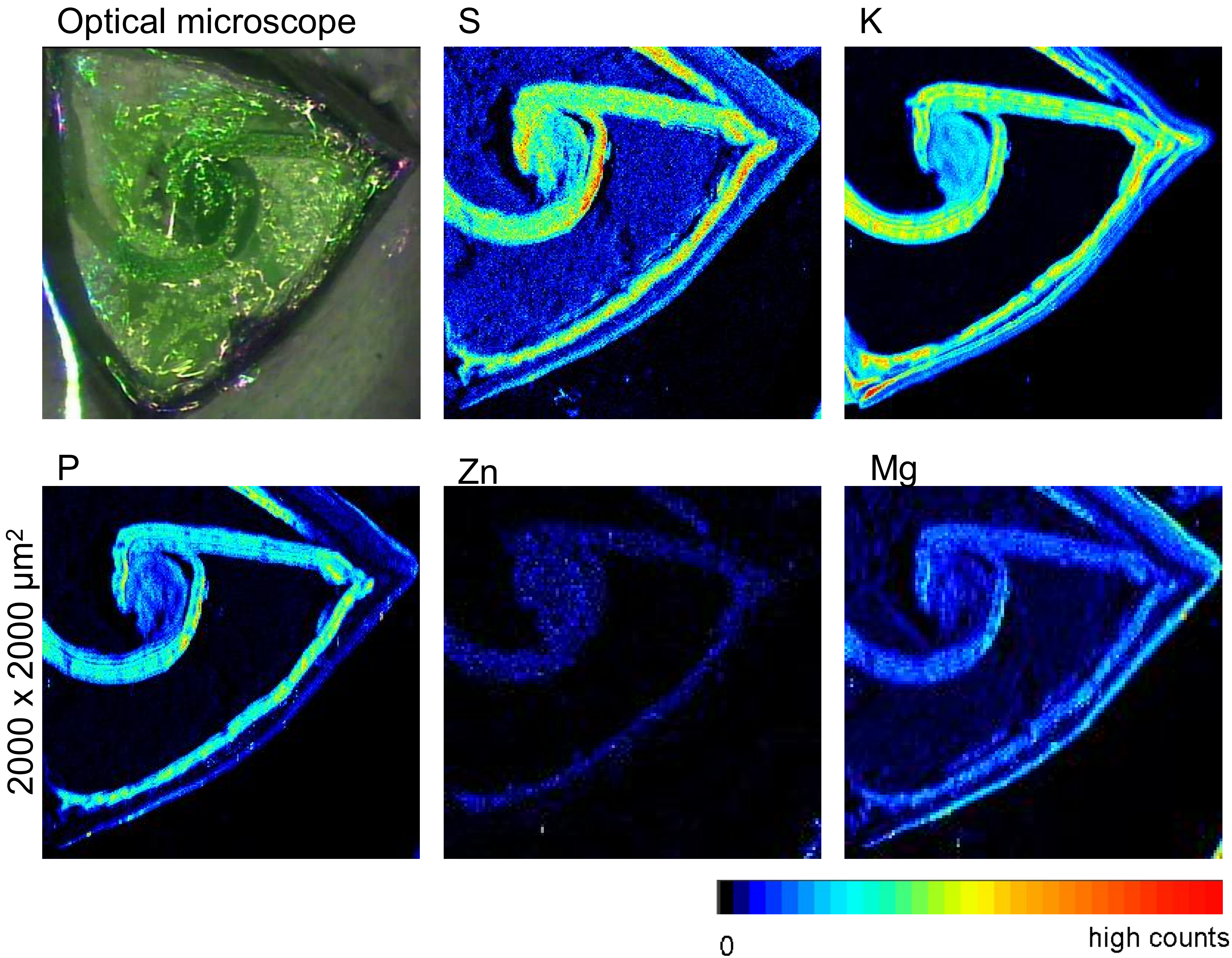

Optical microscope
S
K
P
Zn
Mg
2000 x 2000 µm²
0
high counts

endosperm

Elementi	Konc [ppm]	Stat.err. %	lod [ppm]
Mg	81.9	11.26	16.7
Al	23.7	18.98	8.3
Si	86.3	3.87	5.9
P	78.1	4.73	6.7
S	218.5	1.39	4.9
Cl	63.9	3.53	3.8
K	89.4	2.09	2.8
Ca	68.8	2.39	2.4
Ti	3.9	4.99	3.34E-01
Mn	5.87E-01	17.93	1.81E-01
Fe	13.1	1.63	1.45E-01
Ni	2.13E-01	45.09	1.68E-01
Cu	1.1	11.6	1.52E-01
Zn	6.82E-01	20.74	1.99E-01
Br	2.3	20.72	4.24E-01
Rb	n.d.	0	2.4
Mo	n.d.	0	7.8

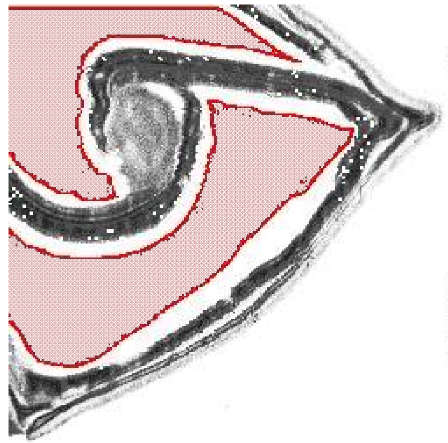

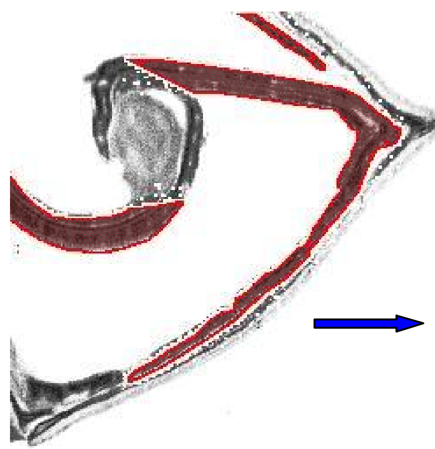

cotyledon

Elements	Konc [ppm]	Stat.err.%	lod [ppm]
Mg	4168.8	0.7	39.6
Al	100.9	14.34	25.4
Si	n.d.	0	47.4
P	10323.9	0.22	23
S	2571.5	0.46	12
Cl	360.8	1.82	9.7
K	10160.5	0.21	12.5
Ca	232.9	8.78	37.7
Ti	3.5	11.04	6.98E-01
Mn	16.2	3	6.83E-01
Fe	45.9	1.8	1.1
Ni	7.15E-01	34.42	4.32E-01
Cu	4.7	8.29	5.34E-01
Zn	40.5	2.38	3.37E-01
Br	n.d.	0	2.9
Rb	n.d.	0	5.3
Mo	n.d.	0	16.3

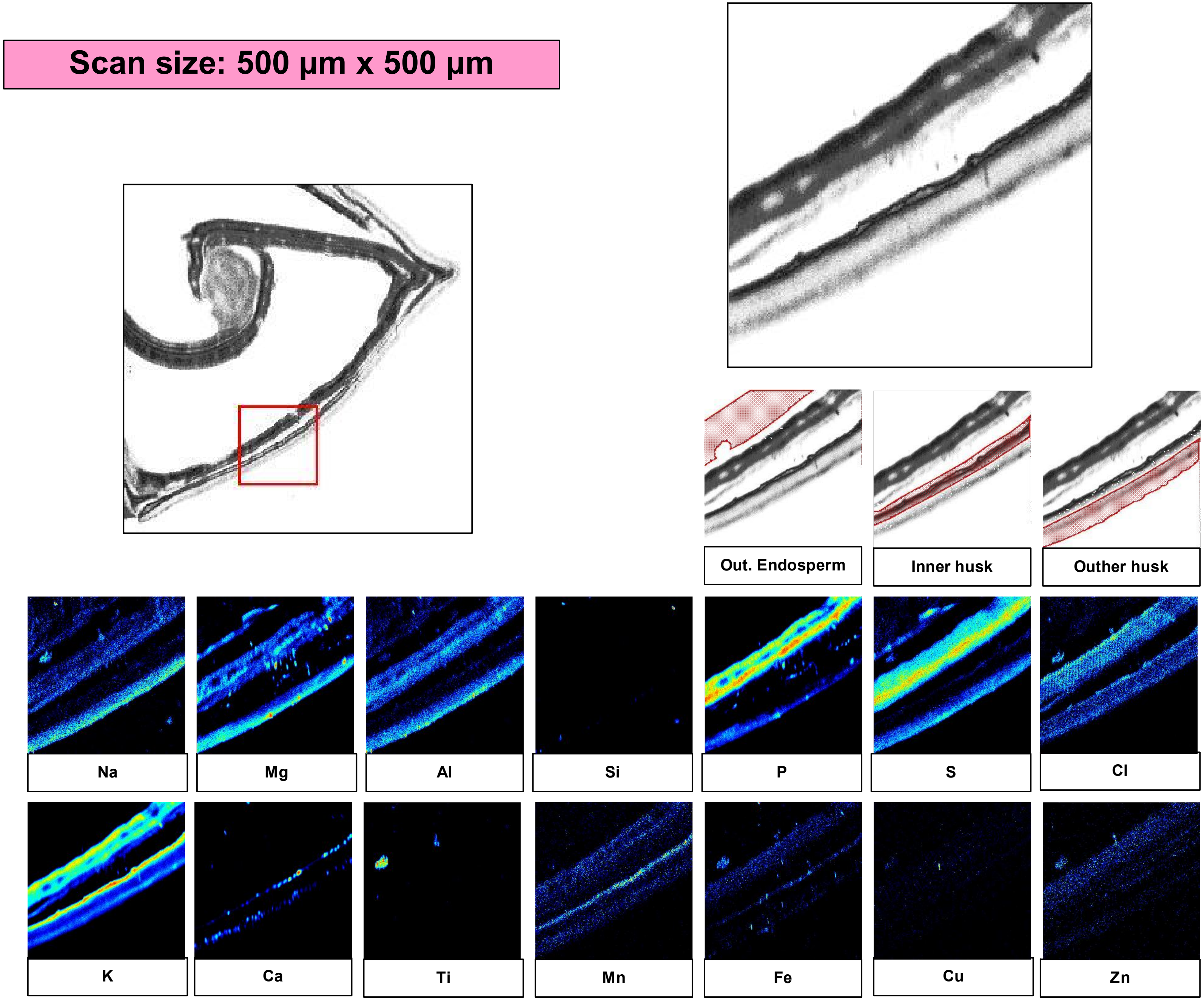
Scan size: 500 µm x 500 µm
Out. Endosperm
Inner husk
Outher husk
Na
Mg
Al
Si
P
S
Cl
K
Ca
Ti
Mn
Fe
Cu
Zn

Wounded beech branch

Radial section of the wounded beech branch. The affected tissue is walled-off from the underlying sound wood. Blue-colored map: Two-dimensional distribution of K over the indicated area of the sample. Lower graphs: measured PIXE concentration of K, Ca, Mn, Fe and Rb as a function of horizontal displacement over the reaction zone. Relative error of measured concentration, determined by GUPIXWIN: K and Ca 5%, Mn and Fe 20%, Rb 40%.W – wound, D – dehydrated tissue, S – sound wood. Scale bar is 5 mm. (Merela et al. in print NIMB).

Arabidopsis roots, Uranium treated

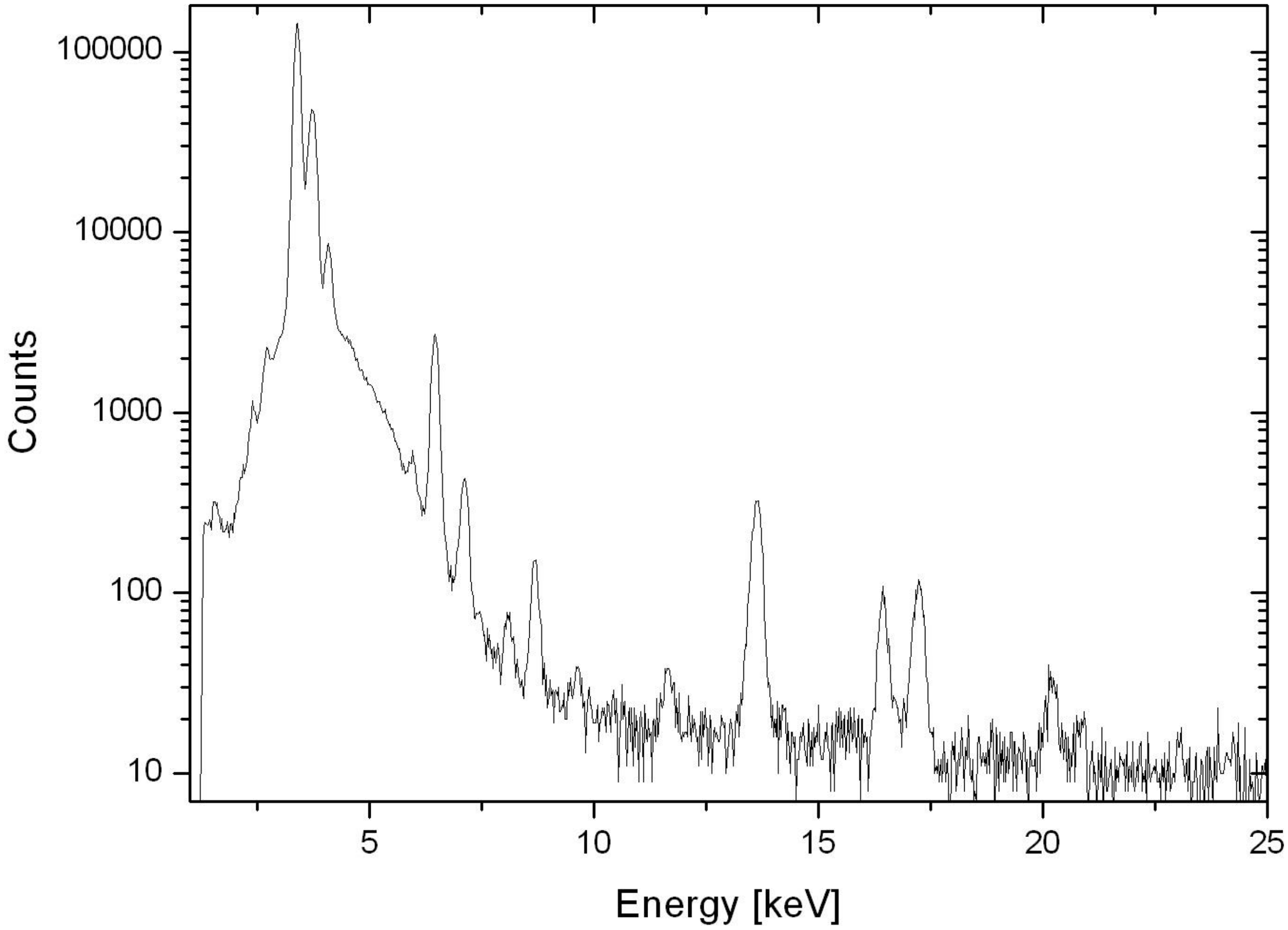

Arabidopsis roots, Uranium treated

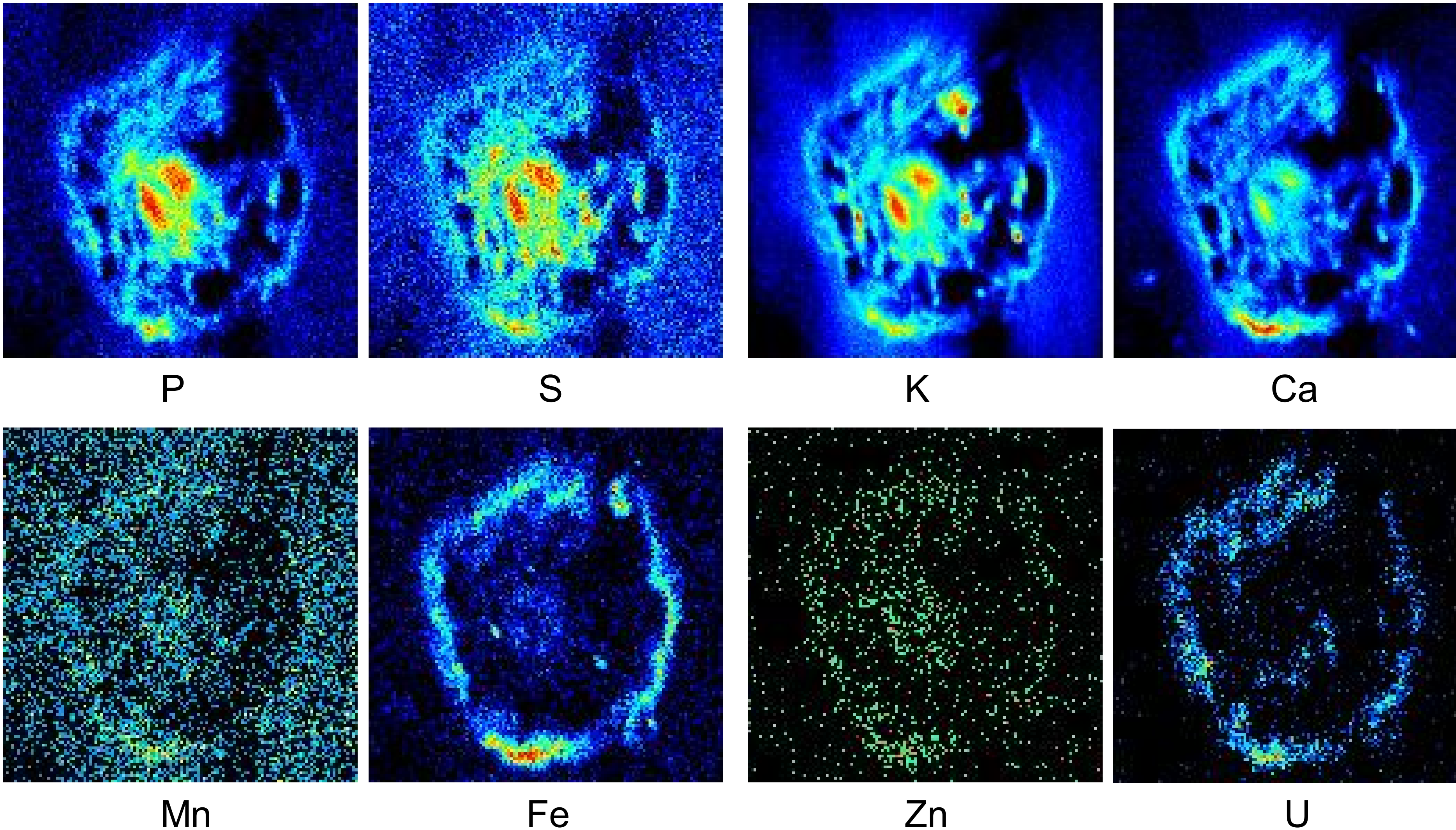

Human tissue, not prepared for PIXE

Hypophysis and kidney tissue of the miner working all his working period in mercury mine without any pathological symptoms was sliced, pathologically examined and stored in a depot.

Years later, they try to gain more info on the tissue elemental composition. It was brought in our lab for PIXE analysis. Tissue was not prepared according to the procedure for micro-PIXE, was of uneven thickness and irregular shape. Protons of 3 MeV penetrated the tissue, intermediate thickness, STIM measurement for exit energy.

Kidney tissue did not show any Hg contamination (concentration bellow L.O.D of 10 ppm).
Hypophysis, however, showed high concentration of Hg of over 200 ppm!

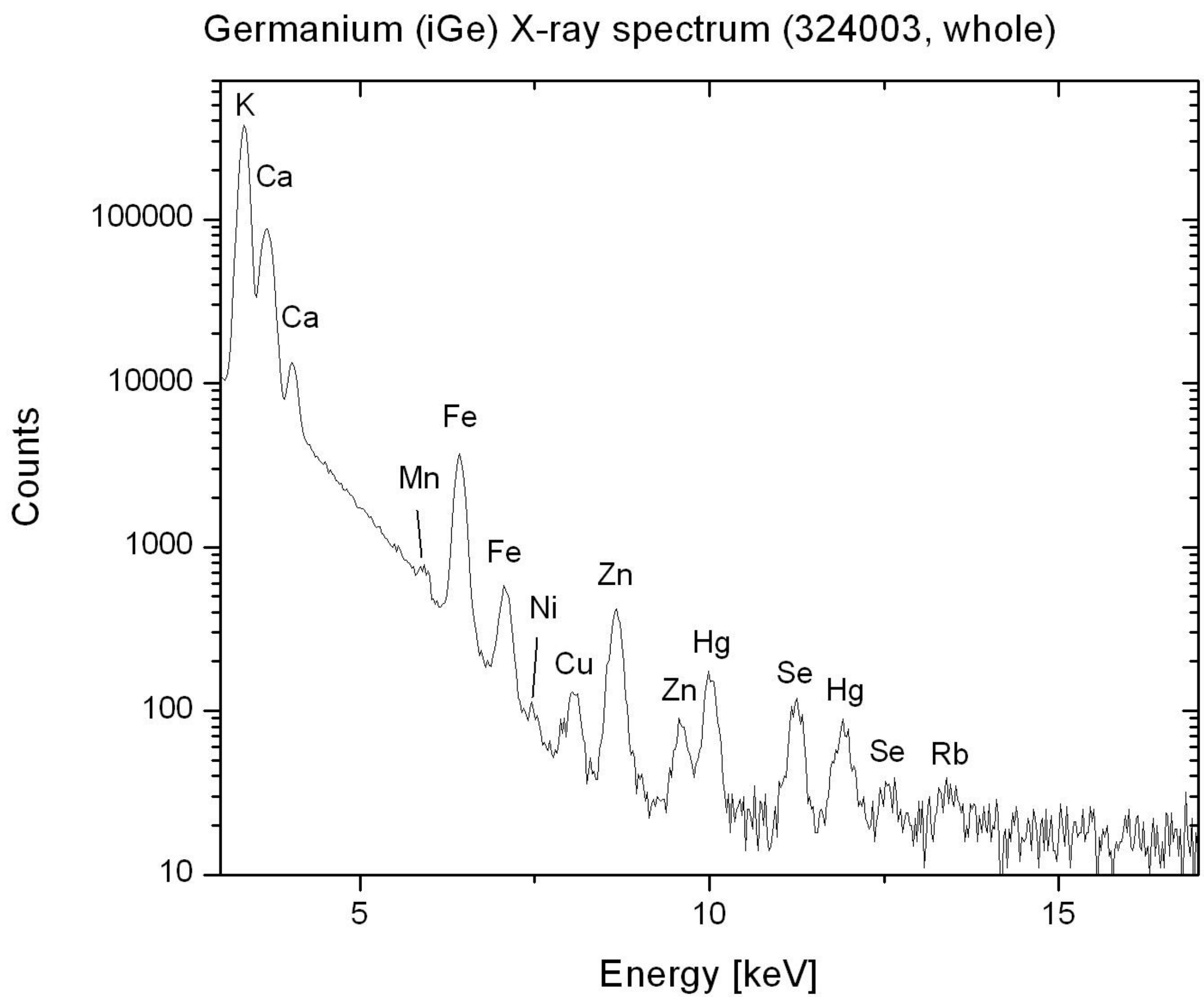
Germanium (iGe) X-ray spectrum (324003, whole)
Counts
Energy [keV]
10
100
1000
10000
100000
5
10
15
K
Ca
Ca
Mn
Fe
Fe
Ni
Cu
Zn
Zn
Hg
Hg
Se
Se
Rb

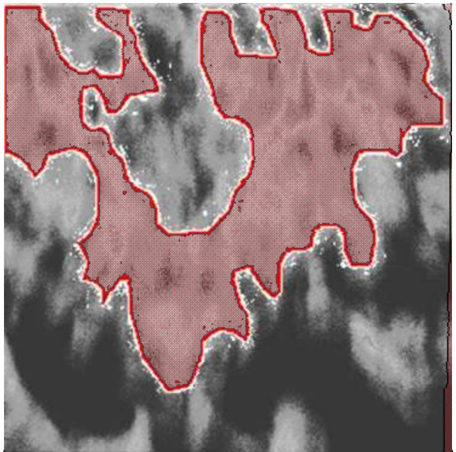

STIM map, cut of consistent tissue part

Elementi	Konc [ppm]	Stat.err.%	lod [ppm]
K	13453.5	0.08	7.8
Ca	1949.4	1	34.3
Mn	12.3	12.22	2.8
Fe	310.4	0.77	2.2
Ni	3.8	25.5	1.7
Cu	16.6	7.37	2.0
Zn	94.2	2.17	1.5
Se	90.1	4.64	3.8
Rb	24.1	28.1	12.3
Hg	229.0	3.58	7.7

Measured Se and Hg concentrations of 90 ppm and 229 ppm, respectively, result in stoichiometry ratio of app. 1:1. Selenium probably play a significant role in Hg toxicity deactivation !

Thank you for your attention

Acknowledgement

The work is supported by the research project J7-0352 and research program P1-0112 of Slovenian Research Agency (ARRS). Support of fusion research within Association Euratom-MHEST is acknowledged. Accelerator facility is funded by ARRS as Infrastructure Reasearch Centre. Accelerator facility and microprobe were built with substantial support of IAEA in the frame of TCP SLO/1/003 and TCP SLO/1/004.